

# BLOOD DAMAGE PREDICTION CONSIDERING VAD'S ROUGH SURFACE BY DISCRETE POROSITY ROUGHNESS METHOD

JITENDRA KUMAR<sup>1</sup>, DUC DUONG VIET<sup>1</sup> AND FRANK-HENDRIK WURM<sup>1</sup>

<sup>1</sup>University of Rostock  
Albert-Einstein-Straße 2, 18059 Rostock, Germany  
Email: jitendra.kumar@uni-rostock.de, duc.viet@uni-rostock.de, hendrik.wurm@uni-rostock.de  
Web page: www.itu.uni-rostock.de

**Key words:** blood damage, VAD, roughness modelling, Discrete Porosity Method.

**Abstract.** Numerical simulations in framework of RANS are carried out for blood damage prediction on a ventricular assist device. The inlet guide vane of an axial blood pump is simplified to a channel flow. The results are compared between smooth and rough channel walls, for which the roughness is considered by Discrete Porosity Method on one channel wall. Thus, a porosity property is associated to selected fluid cells according to Darcy-Forchheimer equations in OpenFOAM. Because of the roughness consideration, viscous shear stress changes locally which leads to different blood damage behavior while the velocity profile is mostly unaffected. The change in blood damage is shown in the results.

## 1 INTRODUCTION

Ventricular assist devices (VAD) find application for patients with a heart insufficiency. A continuous-flow VAD as rotary pump is a promising technical solution [1], but blood damage prediction is required to investigate its hemocompatibility. In the past, most investigations regarding blood damage considered smooth walls [2, 3]. Nevertheless, surface roughness features of the pump affects the viscous shear stress field locally and it may lead to activation of platelets, hemolysis, thrombosis or thromboembolic events (stroke). Watanabe *et. al.* investigated experimentally the influence of surface roughness on shear induced hemolysis [4]. They have found out a correlation between the surface roughness and induced hemolysis. Therefore, investigations are necessary to describe the influence of roughness features on the blood, which will help to decide an appropriate manufacturing process of VADs.

Local roughness features of the surface must be modelled precisely in the numerical roughness model to calculate the local viscous shear stress accurately. Equivalent sand grain height (ESG) model proposed by Nikuradse [5, 6] is still state of the art to consider roughness. However, it can provide global roughness effects like total pressure loss or decrease of velocity in logarithmic wall function, but not the effect on the local shear stress because of roughness features. Body conforming mesh simulations are most common in computational fluid dynamics (CFD) and would provide appropriate results [7]. However, irregular random roughness with a height in the order of  $1\mu\text{m}$ , like on VAD surfaces, are mostly impossible to

mesh in a way with acceptable mesh size and mesh quality.

Discrete Porosity Method (DPM) is an alternative roughness model to add local roughness features in simulations without creating a body-conforming mesh, but adding a porosity property to selected cells. A comparison on regular roughness using RANS simulations have shown that body conforming simulation gives most accurate results validated on direct numerical simulation and experiments. However, DPM and ESG are underestimating friction velocity at the rough wall by 25 % and 100 %, respectively, compared to the experimental data [7]. Hence, DPM is the preferred method in this paper and is described in detail in the following chapter.

## 2 NUMERICAL METHOD

### 2.1 Navier-Stokes-Equations

The Navier-Stokes-Equations are the fundamental equations in CFD. It represents the conservation of momentum and is described as follows [6]:

$$\frac{\partial(\rho u_i)}{\partial t} + \frac{\partial(\rho u_i u_j)}{\partial x_j} = -\frac{dp}{dx_i} + \mu \frac{\partial}{\partial x_j} \left[ \left( \frac{\partial u_i}{\partial x_j} + \frac{\partial u_j}{\partial x_i} \right) - \frac{2}{3} \delta_{ij} \left( \frac{\partial u_i}{\partial x_i} \right) \right] + k_i \quad (1)$$

Considering the porosity, the Navier-Stokes-Equations are modified by adding a sink term to reduce the velocity in selected fluid cells:

$$\frac{\partial(\rho u_i)}{\partial t} + \frac{\partial(\rho u_i u_j)}{\partial x_j} = -\frac{dp}{dx_i} + \mu \frac{\partial}{\partial x_j} \left[ \left( \frac{\partial u_i}{\partial x_j} + \frac{\partial u_j}{\partial x_i} \right) - \frac{2}{3} \delta_{ij} \left( \frac{\partial u_i}{\partial x_i} \right) \right] + k_i - S \quad (2)$$

Originally, porosity was used to determine the pressure drop of porous media like sediment [8] or in heat exchangers [9].

### 2.2 Darcy-Forchheimer Equation

The sink term described in Eq. (2) is considered as additional pressure drop. Darcy has derived a relation between pressure drop over a specific length  $L$  and the mean velocity  $u$  in his experiments. He has defined a linear behaviour with hydraulic conductivity  $k_h$  [8]:

$$\frac{\Delta p}{L} = \frac{1}{k_h} u \quad (3)$$

An improved expression known as the Darcy-Forchheimer equation is shown in Eq. (4) [9, 10]. The pressure drop is divided into a viscous term which is linearly dependent on the velocity and an inertial term which depends on the velocity square. These relations can also be seen as friction drag and form drag, respectively. Here,  $u$  is the velocity vector for a three dimensional domain. In the Darcy-Forchheimer equation, it is possible to define different porous properties in each flow direction. Thus, anisotropic behavior can be considered if necessary:

$$S = \mu D u + \frac{\rho}{2} F |u| u; \quad (4)$$

$$S = \begin{pmatrix} \frac{dp}{dx} \\ \frac{dp}{dy} \\ \frac{dp}{dz} \end{pmatrix}; \quad D = \begin{pmatrix} D_x & 0 & 0 \\ 0 & D_y & 0 \\ 0 & 0 & D_z \end{pmatrix}; \quad F = \begin{pmatrix} F_x & 0 & 0 \\ 0 & F_y & 0 \\ 0 & 0 & F_z \end{pmatrix} \quad (5)$$

### 2.3 Discrete Porosity Method on roughness of a VAD

In the DPM, a cartesian grid represents the fluid domain without any consideration of roughness. This leads to excellent mesh quality regarding skewness and minimum angle. To consider the roughness elements, single fluid cells overlapping with the roughness structure are selected to a set of cells. Therefore, during mesh generation the near wall region is relatively fine discretized to resolve the roughness. For VAD rotors, a polished surface is created having roughness heights less than  $2 \mu\text{m}$ . Here, the polished surface is assumed as a sine function with  $2 \mu\text{m}$  amplitude and  $5 \mu\text{m}$  half wave length according to equation (6), where only the positive amplitude is taken into account. Figure 1 shows a two dimensional view of the sine curve, which is constantly extruded in spanwise direction for the 3D simulation. Streamwise direction and height is in x- and y- direction, respectively.

$$y = 2 \mu\text{m} * \sin(0.6283x) \quad (6)$$

In this way, two kinds of cell sets are created in one domain, a fluid cell set and a roughness cell set, see Figure 2. For the fluid cell volume, RANS equations are solved. For roughness cell volume, the sink term according to Darcy-Forchheimer is added to the RANS equations. Here, a nearly infinite sink shall be created to reduce the velocity in the roughness cells to approximately zero. Therefore, all components of the pressure loss coefficients D and F from equation (5) are set to high values of  $D = 10^{12} \text{ 1/m}$  and  $F = 10^{12} \text{ 1/m}^2$ . Here, it is assumed, that the selected roughness cell is blocking the flow completely, even if the area under the sine curve is not filling the complete fluid cell cross section, see Figure 1. An improvement could have been used to consider the volume fraction between roughness cell and fluid cell and additionally the roughness shape. For simplification, it is not included in this paper.

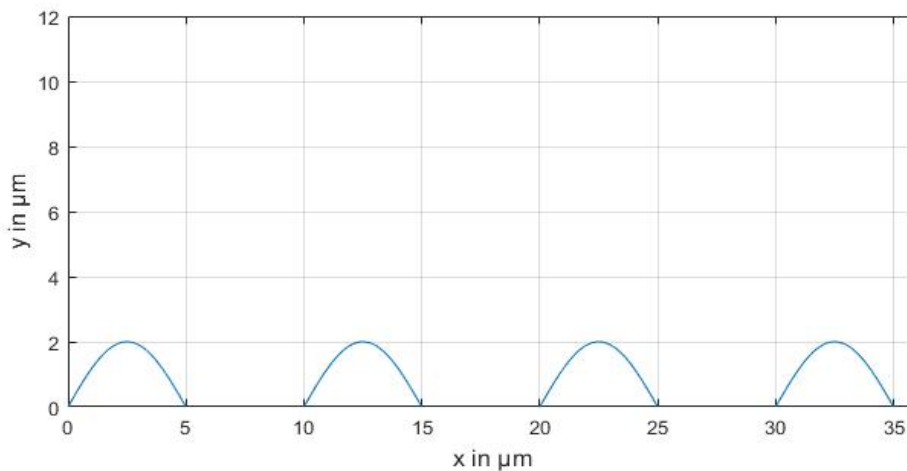


**Figure 1:** Approximation of a polished surface

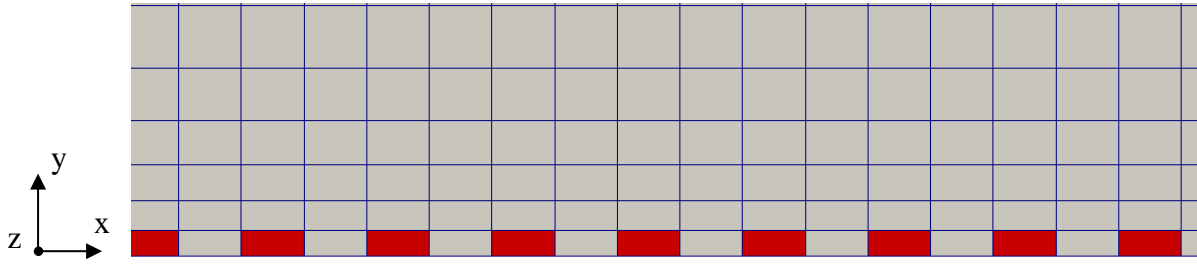


**Figure 2:** Highly zoomed near wall region: fluid cells in grey, roughness cells in red

## 2.4 Computational domain and boundary conditions

An assumed inlet guide vane is simplified to a rectangular channel, see Figure 3 and Figure 4. The channel height is defined as distance between hub and housing resulting in 2 mm. The channel width is defined as arc length between two blades. If the assumed inlet guide vane has a hub diameter of 9.55 mm, the circumference  $C = \pi D$  becomes 30 mm. If three blades are considered, each having 1 mm thickness, the channel width becomes 9 mm. The length of the channel is set to 8 mm. However, primary aim is to compare the roughness effect of VAD's, for which this channel domain length is satisfactory. Moreover, a reduced domain length results in smaller mesh size and reduced computational effort. The overall computational domain has a size of 8x9x2 mm in length, width and height, respectively. In respective directions, the mesh is discretized in 1601x61x71 nodes leading to approximately 7 million nodes. The high discretization in channel length direction is necessary to resolve the roughness elements in streamwise direction, because the sine roughness elements have a distance of 5  $\mu\text{m}$  between each other. In height, the roughness resolution has been maintained by controlling the mesh spacing of the first node from the wall, which is 2  $\mu\text{m}$  according to roughness height. Besides, the roughness in the rough channel is applied on one side only. In this case, the bottom wall is having the roughness. The mesh expansion factor is kept 1.2 for the whole domain. Eventually, the mesh provides good mesh quality regarding skewness and minimum angle reaching 1 and 90°, respectively. Maximum aspect ratio becomes 75 because of the fine discretization in streamwise direction.

Regarding boundary conditions, no slip walls are applied on top and bottom boundary, also for front and back side, see Figure 4. The roughness is applied on the bottom surface as described before. On the outlet, static pressure is set to a fixed value of 0 Pa and the inlet has a defined velocity vector  $(u_x, u_y, u_z)$  giving uniform value of (1.123, 0, 0) m/s. The Reynolds

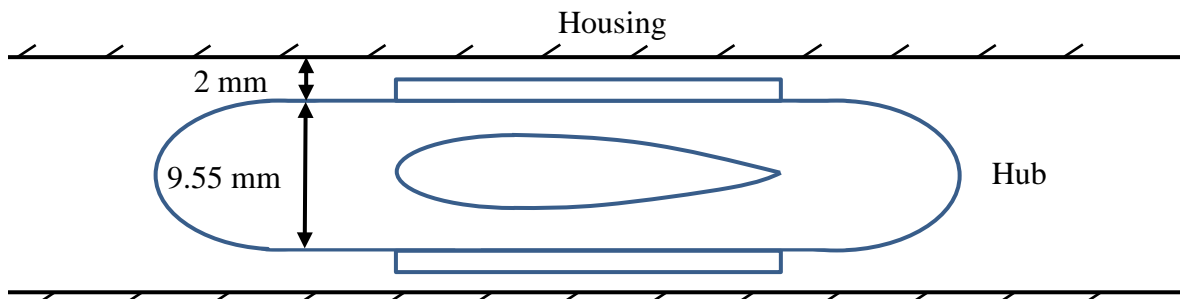


**Figure 3:** Inlet guide vane model for simplification to a rectangular channel

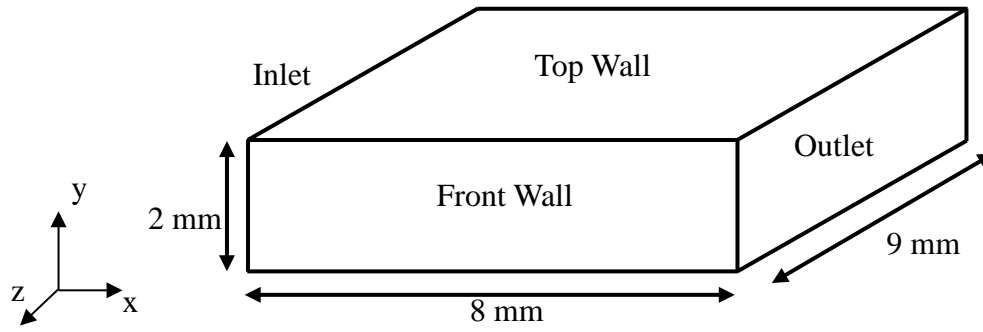


**Figure 4:** Channel dimensions and boundary conditions

number results in  $Re \approx 680$  based on inlet velocity, channel height, blood's density and dynamic viscosity which is  $1050 \text{ kg/m}^3$  and  $0.0035 \text{ Pa s}$ , respectively. The inlet velocity is calculated based on a  $4.5 \text{ l/s}$  volume flow through the inlet guide vane. The resulting Reynold number would lead to a laminar channel flow, but because of inflow conditions of the tube system, turbulence is very probable in reality. Therefore, turbulence settings are applied in a way, that inlet provides a turbulence intensity of 5 %. For steady RANS simulation using simpleFOAM solver, the turbulence model  $k-\omega$ -SST has been used. Moreover, blood is considered as newtonian fluid because its non-newtonian behavior decreases with higher shear stresses. From  $100 \text{ Pa}$  on, there is an no significant change is noticeable [11]. In this simulation, it is valid for the near wall region, which is object of interest in this paper.

Because of an inlet guide vane, no rotational motion is considered here. In addition, the influence of the rotation of the VAD rotor is neglected simplifying the inlet and outlet boundary condition. Here, the channel has a constant width because the blades have an assumed constant thickness. The actual blade channel has a varying width because of the blade's profile. Moreover, top and bottom walls are assumed to have same size, even though the top wall should have a bigger width because of curvature and larger housing radius.

## 2.5 Blood damage

Blood damage can be indicated based on the shear strain rate and resulting shear stress in the domain. Strain rate tensor is written as:

$$S_{ij} = \frac{1}{2} \left( \frac{\partial U_i}{\partial x_j} + \frac{\partial U_j}{\partial x_i} \right) \quad (7)$$

having three scalar invariants, one of them is called shear strain rate [12]:

$$\dot{\gamma} = \left[ 2 \frac{\partial U_i}{\partial x_j} S_{ij} \right]^{\frac{1}{2}} \quad (8)$$

The shear stress is defined by dynamic viscosity and shear strain rate:

$$\tau = \mu * \dot{\gamma} \quad (9)$$

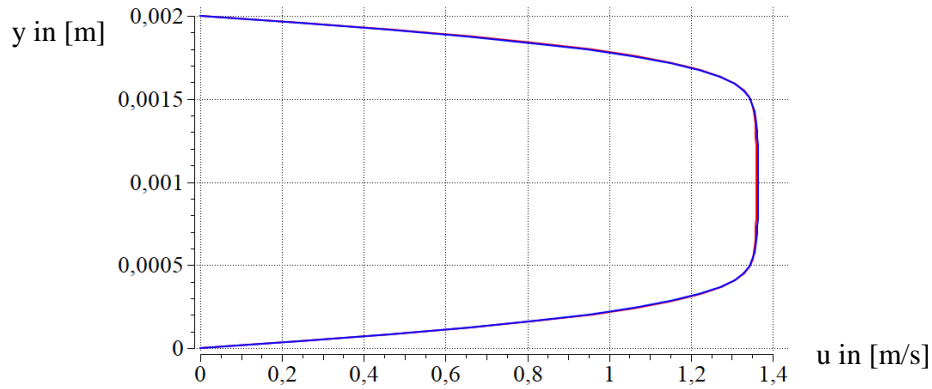


**Figure 5:** Velocity profile  $y$  over  $u$  of smooth channel (blue) and rough channel (red)

Thamsen *et. al.* [13] proposed that protein damage, also called von Willebrand factor cleavage, potentially occurs above a shear stress of 9 Pa. Above 50 Pa platelet activation happens resulting in thrombus formation. Finally, hemolysis starts at shear stress of 150 Pa.

### 3 SIMULATION RESULTS AND DISCUSSION

For comparison, two simulations have been carried out. The first one has considered all walls as smooth walls. The second one has considered the bottom wall as a rough wall according to Discrete Porosity Method. All other boundary conditions remain same.

Basically, if the roughness height is inside the viscous sublayer, the wall will be considered as hydraulically smooth and will not affect the flow [5]. In these simulations, the value of maximum  $y^+$  reached 0.02. According to Schlichting [5], the viscous sublayer ranges until a  $y^+$ -value of 5 which means the first grid point away from the wall is inside the viscous sublayer. Hence, the considered roughness is also in the viscous sublayer, because the mesh has been adapted to the roughness height. The velocity profile with respect to wall normal distance  $y$  is plotted in Figure 5. The vertical line has been set at spanwise center, i.e. 4.5 mm from the sidewalls and 6.5 mm from the inlet. Apart from small difference in centerline velocity, which possibly results from numerical errors, the velocity profiles are equal. However, there is an effect of roughness on the flow concerning blood damage. Because of roughness consideration, the shear strain rate and consequently the shear stress in the rough

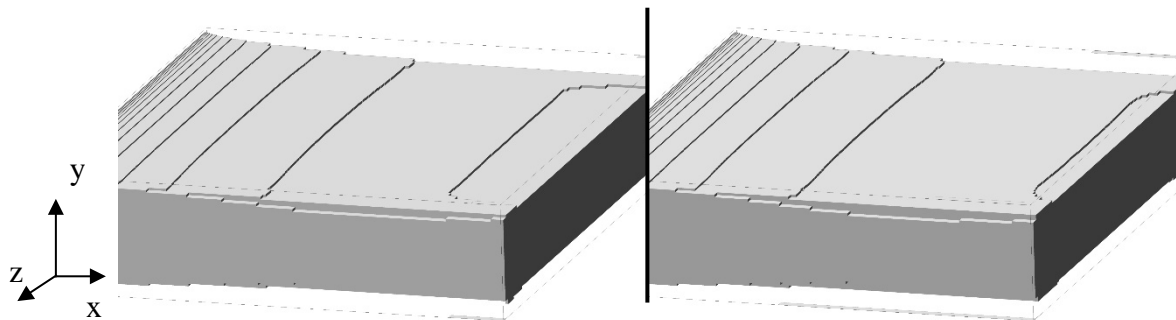


**Figure 6:** Cell volumes of starting protein damage in smooth channel (left) and rough channel (right), activated wire frame of the channel

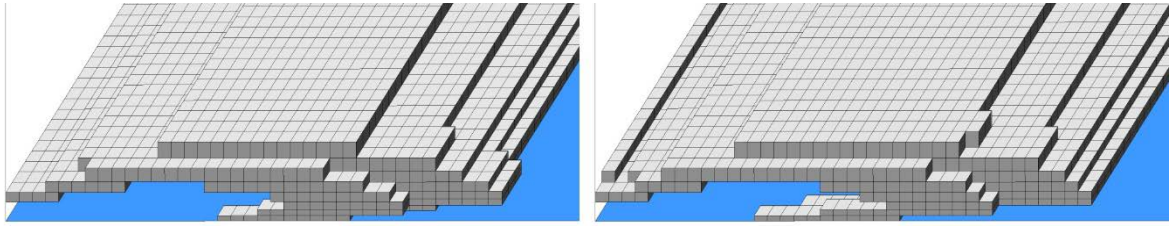


**Figure 7:** Hemolysis starting in cell volumes near the inlet on smooth channel (left) and rough channel (right), activated grid and bottom wall (blue)

channel show higher values in the near wall region than in the smooth channel.

In Figure 6, the displayed cell volumes contain all cells having a shear stress of 9 Pa defining start of protein damage. Certain regions of cell volumes are located closer to the wall in the rough channel simulation, especially seen in the area near the outlet. However, the total volume for rough wall is smaller than for smooth walls in case of protein damage, see Table 1. This could mean, that the core flow has still the same field of low shear, but the region with 9 Pa changes its distribution.

In Figure 7, shear stress above 150 Pa occurred near the inlet, because of boundary layer development, i.e. the boundary layer is small close to the inlet resulting in high shear stresses in this near wall region. With greater boundary layer thickness in streamwise direction, the wall shear stress is decreasing, which is a typical channel flow behavior. For rough walls, more cell volumes with shear stress above 150 Pa can be noted. This behavior can also be seen for platelet activation above 50 Pa. Table 1 summarizes fluid volumes of regions with starting blood damage effects. Besides, all the volumes are relatively small compared to the total domain size, which is  $1.44 \text{ e-}7 \text{ m}^3$ .

**Table 1:** Fluid volumes of starting blood damage regions with limit values according to [13]

	Protein damage	Platelet activation	Hemolysis
Smooth [ $\text{m}^3$ ]	9.354 e-9	4.041 e-10	1.115 e-10
Rough [ $\text{m}^3$ ]	9.335 e-9	4.108 e-10	1.127 e-10
Difference [%]	0.2	1.6	1.1

On the one hand, a difference in blood damage behavior is visible in the simplified channel flow simulation, even though the percentage difference is very small. On the other hand, many effects are neglected here, e.g. the diffusor effect in the blade channel, shape of the blades, rotational effects of the rotor, additional turbulence or swirl because of the tube system before the inlet guide vane. If more of the mentioned effects are additionally modelled, a more realistic shear field can be simulated which would enhance the difference between smooth and rough wall simulation regarding blood damage prediction. Moreover, the inlet guide vane is a stationary, non-rotational part of a VAD. If the rotor would be simulated, even more effects will be considered, for example secondary flows like flow through the clearance between blades and housing, the revolution of the rotor itself leading to an additional velocity component and an increasing pressure along the rotor. This will result into a more advanced and complex flow and shear field.

## 4 CONCLUSION

Steady RANS simulations are performed in OpenFOAM for an inlet guide vane of a VAD for smooth walls and with rough wall consideration of a polished surface of 2  $\mu\text{m}$  roughness height. Therefore, roughness has been modelled by Discrete Porosity Method. The inlet guide vane has been simplified to a channel flow, representing one blade channel. As a result, velocity profiles are matching each other because the roughness height is inside the viscous sublayer, representing a hydraulically smooth wall. However, shear stresses are lightly affected by roughness. The provided results show small, but still noticeable change in blood damage behavior taking roughness into account. More regions of starting platelet activation and hemolysis occur because of roughness consideration. For better blood damage prediction, less assumptions have to be done to consider more physical effects and find more appropriate results.

## REFERENCES

- [1] Maybaum S., Mancini, D., Xydas S., et. al. Cardiac Improvement During Mechanical Circulatory Support, *Circulation* (2007) **115**: 2497-2505.
- [2] Leverett L.B., Hellums J.D., Alfrey C.P. and Lynch E.C. Red blood cell damage by shear stress. *Biophys. J.* (1972) **12**: 257-273.
- [3] Heuser G, Opitz R. A Couette viscometer for short time shearing of blood. *Biorheology J.* (1980) **17**:17-24.
- [4] Watanabe N., Ueda S., Nagashima K., Oguri T. and Mita T. Ratio of surface roughness to flow scale as additional parameter for shear-induced hemolysis. *Int. J. Artif. Organs* (2016) **39**: 205-210.
- [5] Nikuradse J. Laws of flows in rough pipes. *NACA Technical Memorandum 1292* (1950).
- [6] Schlichting H. and Gersten K. *Boundary-Layer Theory*, Springer-Verlag, 8<sup>th</sup> Edition (2000).
- [7] Duong Viet D., Kumar J., Wurm F.H. Discrete Porosity Method for Roughness Modelling in the Framework of RANS. *Proc. MCM'17*, (2017) Paper No: HTTF 118.
- [8] Darcy H., *Les fontaines publiques de la ville de Dyon*. Victor Dalmont, Paris (1856).
- [9] Missiris D., Donnerhach S., Seite O., Albanakis C., Sideridis A., Yakinthis K. and Goulas A. Numerical development of a heat transfer and pressure drop porosity model for a heat exchanger for aero engine applications, *J. of Applied Thermal Eng* (2010) **30**:1341-1350.
- [10] Dupuit A.J.D.J. *Etudes Theoriques et Pratiques sur le mouvement des eaux dans les canaux decouverts et a travers les terrains permeables*. Victor Dalmont, Paris (1963).
- [11] Merrill E.W., et. al. Rheology of Blood nad flow in the microcirculation. *J. Appl. Physiol.* (1963) **18(2)**: 255-260.
- [12] ANSYS Documentation CFX, *Release 18.0., Help System, Theory Guide, Variable Definitions*, ANSYS, Inc.
- [13] Thamsen B., Blumel B., Schaller J., Paschereit C.O., Affeld K., Goubergrits L., Kertzscher U. Numerical Analysis of Blood Damage Potential of the HeartMate II and HeartWare HVAD Rotary Blood Pumps. *J. Artif. Org.* (2015) **39**: 651-659.